GPS Solutions (2024) 28:107
https://doi.org/10.1007/s10291-024-01612-y

ORIGINAL ARTICLE

Construction of a meteorological application system based on BDS ground-based augmentation network and water vapor products validation

Mingbin Du[1,5] · Yunchang Cao[2] · Hong Liang[2] · Heng Hu[2] · Haishen Wang[2] · Shuli Song[3] · Guoqiang Jiao[4]

Received: 4 July 2023 / Accepted: 12 January 2024

Abstract
The national Beidou Navigation Satellite System (BDS) ground-based augmentation network (BGAN) of China is constructed with the existing GNSS observation resources of industrial sectors and local governments, based on the concept of joint building and sharing with sustainable development. This study provides a detailed introduction to the design, construction and operation of a meteorological application system based on BGAN, and validation of its water vapor products. BDS and GPS real-time observation of atmospheric water vapor is achieved nationwide in China and multi-GNSS applications. Through the application of multi-GNSS data and validation of the water vapor products from 2018 to 2020, the accuracy of precipitable water vapor (PWV) derived from BDS only is equivalent to that from GPS only. The root mean square error (RMSE) between them is about 2 mm with high correlation coefficient. Based on radiosonde data, the validation is conducted with the products of BDS-PWV, GPS-PWV, and Combined-PWV derived with multi-GNSS of BDS and GPS. The error characteristics of the three products show a consistent trend over the months. The bias is relatively small. The RMSE of the three products is in the range of 2.18–2.73 mm. The BDS-PWV has the largest RMSE, followed by GPS-PWV, and Combined-PWV has the smallest RMSE.

Keywords BDS · Ground-based augmentation · Multi-GNSS · PWV · GPS

Introduction

The Beidou Navigation Satellite System (BDS) is the third mature international Global Navigation Satellite System (GNSS), following GPS and GLONASS. The national BDS ground-based augmentation network (BGAN) of China is an important infrastructure that uses differential correction techniques to improve navigation accuracy, integrity, continuity, and other service performance by building a Continuously Operating Reference System (CORS) with known precise coordinates (Pinker et al. 2000; Kee et al. 2004). This is globally recognized as a reliable means for the high-quality development of GNSS services (Li et al. 2015a; Federal Aeronautics Administration 2017; Jones et al. 2020). The construction and application of a Meteorological Application System based on BGAN can effectively improve the GNSS/MET observation quality, and support both the development of China's meteorology and BDS industrialization.

Traditional means of atmospheric water vapor monitoring, such as radiosonde, microwave radiometer and surface weather station, have a number of drawbacks,

✉ Mingbin Du
nyicer@hotmail.com

✉ Yunchang Cao
caoyc@126.com

✉ Hong Liang
liangh@cma.gov.cn

1 Shanghai Meteorological Service, Shanghai 200030, China

2 Meteorological Observation Center of China Meteorological Administration, Beijing 100081, China

3 Shanghai Astronomical Observatory, Chinese Academy of Sciences, Shanghai 200030, China

4 Beijing Institute of Tracking and Telecommunication Technology, Beijing 100094, China

5 Shanghai Ecological Forecasting and Remote Sensing Center, Shanghai 200030, China

Published online: 22 April 2024

such as insufficient spatial or temporal resolution, limited accuracy, influenced by weather or restricted application. The ground-based GNSS observation of water vapor has the advantages of low cost, high accuracy and no need for calibration, and is a powerful complement to traditional means of atmospheric water vapor observation (Zhang et al. 2019; Jones et al. 2020). In recent years, China's GNSS/MET operational network has grown to a significant scale. With the rapid development of national and local GNSS networks, China Meteorological Administration (CMA) has built about 1200 ground-based GNSS stations through the construction such as Meteorological Monitoring and Disaster Warning Project and the Crustal Movement Observation Network of China (CMONOC), as well as integrated networks at different levels of local government (Liang et al. 2015; Li et al. 2018; Zhang et al. 2019). The network is usually built jointly with government agencies such as seismology, surveying and mapping, the Chinese Academy of Sciences. These stations are operated in real-time, covering the whole country. Based on radiosonde data, the accuracy of real-time operational Precipitable Water Vapor (PWV) derived from GPS data in China is about 3 mm, with a Relative Error (RE) of about 12% (Jiang et al. 2014; Liang et al. 2015). In the BDS meteorological applications, PWV was retrieved in 10 stations of the Asia–Pacific region of 2013, and the Standard Deviation (Stdev) is about 2.5 mm for both BDS-PWV and GPS-PWV, respectively, while the RMSE of BDS-PWV compared to GPS-PWV is about 2 mm (Li et al. 2015a). It can be seen that the accuracy of PWV derived with BDS is comparable to that with GPS (Li et al. 2015c, 2018; Guo et al. 2020). A strong correlation is found between BDS-PWV and GPS-PWV with a correlation coefficient about 0.95 (Li et al. 2018).

Studies have shown that multi-GNSS increases the number of observable satellites, enhances the satellite positioning geometry configuration, and outperforms single systems in terms of positioning accuracy, availability, and continuity (Xu et al. 2013; Prange et al. 2017; Kazmierski et al. 2020). The combination of multi-GNSS has become a trend in GNSS navigation and positioning. The positioning performance of multiple BDS/GPS/GLONASS system combinations has been analyzed and compared, and the combined GPS/BDS result shows more efficiency improvement (Lou et al. 2016). Additionally, it is noted that the combined GPS/BDS results show the best performance in the Asian–Pacific region which is in the coverage of BDS service at that time. Bu et al. (2021) assesses the individual GNSS (GPS, BDS, GLONASS, Galileo and QZSS) and the combined solutions, and indicates that the measurements based on BDS/GPS combination is significantly better than that of other combination schemes. Multi-GNSS provides more tropospheric delay observation information, and GNSS water vapor monitoring is transitioning from a single system to a multi-system in meteorological application (Li et al. 2015c; Chen et al. 2021; Jones et al. 2020). The GPS and BDS observations during the first half year of 2014 are processed for real-time PWV retrieval, and the results of 5 stations show that the RMSE of the PWV differences are 1.5–1.8 mm for the combined BDS and GPS solution, 1.7–2.1 mm for the GPS-only solution, and 2.4–2.8 mm for the BDS-only solution, compared with nearby radiosonde observations of distance < 50 km (Lu et al. 2015).

The BDS has achieved global coverage with the development and modernization in recent years (Chen et al. 2021; Geng et al. 2024), and it commands more attention to the application in various application fields, compared to the GPS and GLONASS which have been fully operational for a long time. A lot of work has been done in the meteorological application with BDS and combination with other GNSSs. However, the construction of large-scale regional networks and long sequence observations of BDS and synchronous multi-GNSS are still insufficient. The construction of a Meteorological Application System based on BGAN carries out meteorological applications by bringing together the functions of network planning, data management, product generation and distribution, visual display and analysis, etc., and realizes the integration of the BGAN with the GNSS/MET operational network of CMA. This study focuses on constructing a Meteorological Application System based on BGAN and the technology for applying multi-source GNSS data. The general design principles, the technical route and the ways to achieve them are introduced in detail. The combination of multi-GNSS data is carried out, as well as validation of its water vapor products. And the issues related to the construction and application technology are analyzed and discussed.

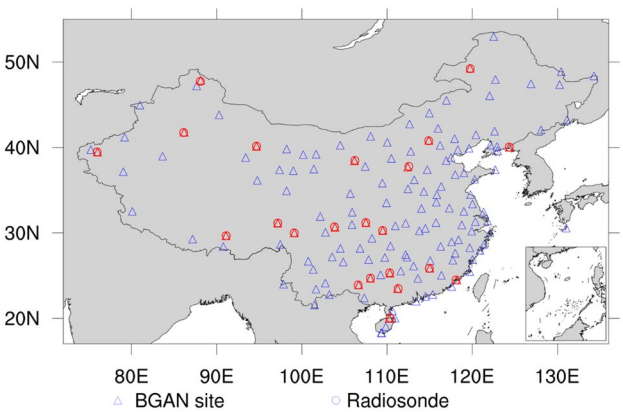

Fig. 1 Sites of BGAN in China and surrounding areas. The collocated sites are shown in red with radiosonde

BDS ground-based augmentation network

BGAN is an important ground-based infrastructure for BDS, as shown in Fig. 1, which aims to meet the user needs through the auxiliary technology with the ground-based reference networks, so that the user navigation accuracy, integrity, continuity and availability can be improved. The overall system is prepared by the National Weapons Industry Corporation of China, and is jointly undertaken by the Ministry of Transport, the State Bureau of Surveying and Mapping, CMA, the Chinese Academy of Sciences and other agencies of China. The Meteorological Observation Center of CMA is responsible for the construction of the meteorological application system based on BGAN. High precision and resolution water vapor and ionosphere products are obtained by receiving and processing data from 175 BGAN stations, combined with the current GNSS/MET operational network of CMA. The system achieves the exchange of the existing GNSS/MET operational network of CMA and the national integrated data processing center of BGAN, with a data communication system and processes BGAN data to retrieve high-precision products. It is beneficial for the mitigation of meteorological disasters and global response to climate change and promotes the high-quality development of BDS application in meteorology combined with other GNSS.

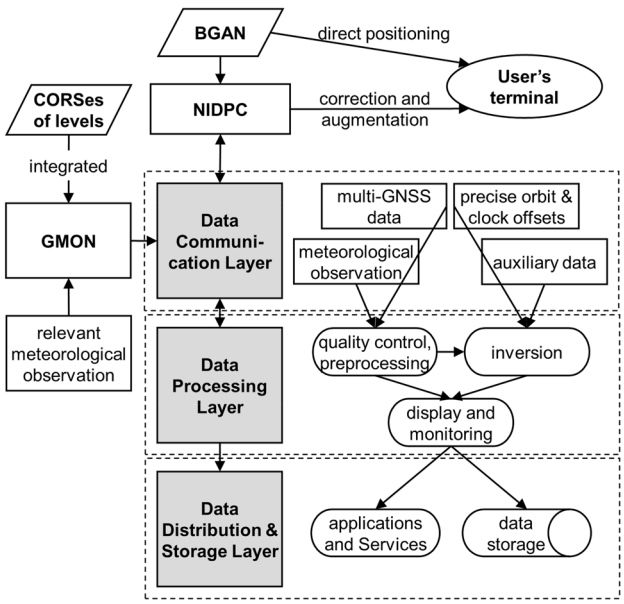

Fig. 2 Frame design of the Meteorological Application System based on BGAN, where GMON is GNSS/MET operational network; NIDPC is National integrated data processing center. The shaded boxes represent the infrastructure of the application system, for implementing data communication, processing, and services, respectively. The arrows denote processing sequences

Architecture design

The architecture design of the Meteorological Application System Based on BGAN follows business logic requirements, and the system is composed of three layers, as shown in Fig. 2: data communication layer, data processing layer, and data distribution and storage layer. The data communication layer realizes the connection between the GNSS/MET operational network and the national integrated data processing center of BGAN, with collecting GNSS data at all levels and relevant meteorological observation. The data processing layer implements quality control, preprocessing multiple GNSS data, meteorological observation, precise ephemeris, retrieving meteorological products with multi-GNSS solution, and realizing product display and monitoring. The data distribution and storage layer is responsible for serving and supporting the operational and scientific applications of BDS in the meteorological service.

Main functions and key solutions

This section presents main functions and strategy of the meteorological application system based on BGAN. The ground-based GNSS/MET uses navigation satellite data to calculate the Zenith Total Delay (ZTD) and then separates Zenith Hydrostatics Delay (ZHD) with meteorological data. The difference between ZTD and ZHD is the Zenith Wet Delay (ZWD), and then PWV can be derived with ZWD and the conversion function. Therefore, the key solutions include real-time data communication and processing, multi-GNSS combination for ZTD estimation, and the subsequent PWV inversion.

Real-time data communication

A 10 M + 2 M dual-link fiber network has been established to realize the communication between the GNSS/MET operational network and the national integrated data processing center of BGAN, as shown in Fig. 2. The open shortest path first (OSPF) protocol is employed to define different verification methods for areas, and exchange information through interactive verification of routes, improving the security of data communication process effectively. BGAN is comprised of 175 reference stations, 35 of which were built by the CMA. The real-time data communication has enhanced and integrated the existing ground-based GNSS/MET network, which is conducive for building an intensive application system, establishing unified data application standards, and improving data application efficiency.

Data processing for meteorological service

As shown in Fig. 2, data processing includes real-time monitoring and meteorological products inversion, and the functions are deployed in the real-time monitoring area and core operation area, respectively. The real-time monitoring area realizes functions such as data reception monitoring, product monitoring, system monitoring, and fault alarm. The core operation area achieves real-time processing of data from 175 BGAN stations nationwide and about 1000 GNSS/MET stations of the CMA operational network. Water vapor products are retrieved to meet the needs of weather observation and prediction.

The key technique in data processing is the solution to combining multi-GNSS of BDS and GPS. In the water vapor inversion with a multi-GNSS solution, BDS and GPS share a common tropospheric zenith delay parameter. Compared to a single GNSS system, combination processing can theoretically improve the accuracy and reliability of calculation by adding redundant observations. However, multi-GNSS of BDS and GPS data combination must consider the impact of different hardware delay biases between different systems, and usually all computed biases of other system are obtained relative to the biases for the GPS observations.

Solution for combining multi-GNSS of BDS and GPS

The commonly used GNSS-PWV solutions include Precise Point Positioning (PPP) and network Double Difference (DD) modes (Li et al. 2015b; El-Mowafy et al. 2016). The PPP mode utilizes precise orbit and clock offsets to obtain ZTD directly, which is superior to the DD mode in terms of observation requirement and computation efficiency. For real-time PPP processing, precise orbit and clock offsets have to be determined first using the observation data from ground-based GNSS network. With the development of GNSS, International GNSS Service (IGS) began the Multi GNSS Experiment (MGEX) project in 2012, and multi-system orbit and clock offsets products are provided (Montenbruck et al. 2017; Prange et al. 2017). The international GNSS Monitoring and Assessment System (iGMAS) is proposed and initiated by China in order to track multi-GNSS satellites and serve global GNSS users as a platform with satellite orbit, clock, station coordinates, and kinds of products (Cai et al. 2016; Mota et al. 2019; Chen et al. 2021). In this contribution, the precise ephemeris and auxiliary data are from the iGMAS.

With the development of GNSS, PPP mode has become an important development trend in the application of multi-GNSS combinations. A lot of GNSS meteorological applications have confirmed that the two processing modes provide ZTD results with similar quality (Xu et al. 2013; Li et al. 2015a; Jones et al. 2020). Generally, in order to eliminate the first-order effect of the ionosphere, the ionosphere-free combination of dual-frequency carrier phase and pseudorange are used in PPP processing (Zhang et al. 2016; Lou et al. 2016; Bu et al. 2021). With satellite orbit, satellite clock, station position, and model correction such as phase center offset, solid tide, phase wind-up, relativistic effects, the combined observation equation can be expressed as follows (Kouba 2009; Jiang et al. 2015; Li et al. 2015b).

$$\begin{cases} P_r^C = \rho_r^C + c\left(dt_r - dt^C\right) + c(d_{rC} - d^C) + m_r^C \cdot zt\mathrm{d}_r + \varepsilon_{r,P}^C \\ P_r^G = \rho_r^G + c\left(dt_r - dt^G\right) + c(d_{rG} - d^G) + m_r^G \cdot zt\mathrm{d}_r + \varepsilon_{r,P}^G \\ \phi_r^C = \rho_r^C + c\left(dt_r - dt^C\right) + \lambda_C(b_{rC} - b^C) + m_r^C \cdot zt\mathrm{d}_r + \lambda_C N_r^C + \varepsilon_{r,\phi}^C \\ \phi_r^G = \rho_r^G + c\left(dt_r - dt^G\right) + \lambda_G(b_{rG} - b^G) + m_r^G \cdot zt\mathrm{d}_r + \lambda_G N_r^G + \varepsilon_{r,\phi}^G \end{cases} \tag{1}$$

where C and G represent BDS and GPS satellites, respectively, and r is the receiver; P is the pseudorange, ϕ is the phase observation; ρ is the geometric distance between the GNSS station and the satellite; dt_r, dt^C and $\mathrm{d}t^G$ represents the clock offset of receiver, BDS and GPS; c is the speed of light in vacuum; m indicates the global mapping function (Böhm et al. 2006; Geng et al. 2012); λ is the wavelength of the observation phase observed; N is the phase ambiguity; d_{rC} and d_{rG} are the code hardware biases of the receiver for BDS and GPS, respectively; d^C and d^G are the code hardware biases of the satellite of BDS and GPS; b_{rC} and b_{rG} are the phase hardware biases of the receiver for BDS and GPS, respectively; b^C and b^G are the phase hardware biases of the satellite of BDS and GPS, respectively; ε is usually the observation noise and multipath effect lumped together. Usually, the receiver clock offset and code hardware bias cannot be separated, and the code hardware bias of GPS is artificially set to 0 in order to eliminate the singularity between receiver clock and code bias parameters (Zhang et al. 2016; Li et al. 2015b), and the estimated signal code bias between BDS and GPS is inter-system bias (ISB). To simplify the formula, (1) can be expressed as follows.

$$\begin{cases} P_r^C = \rho_r^C + c\left(\tilde{dt}_r - \tilde{dt}^C\right) + m_r^C \cdot ztd_r + \varepsilon_{r,P}^C + c \cdot ISB_r \\ P_r^G = \rho_r^G + c\left(\tilde{dt}_r - \tilde{dt}^G\right) + m_r^G \cdot ztd_r + \varepsilon_{r,P}^G \\ \phi_r^C = \rho_r^C + c\left(\tilde{dt}_r - \tilde{dt}^C\right) + m_r^C \cdot ztd_r + \lambda_C \tilde{N}_r^C + \varepsilon_{r,\phi}^C + c \cdot ISB_r \\ \phi_r^G = \rho_r^G + c\left(\tilde{dt}_r - \tilde{dt}^G\right) + m_r^G \cdot ztd_r + \lambda_G \tilde{N}_r^G + \varepsilon_{r,\phi}^G \end{cases} \tag{2}$$

$$\begin{cases} \tilde{\mathrm{d}}t_r = \mathrm{d}t_r + d_{rS} \\ \tilde{\mathrm{d}}t^S = \mathrm{d}t^S + d^S \quad , S = \{C, G\} \\ \tilde{N}_r^S = N_r^S + b_{rS} - b^S \end{cases} \tag{3}$$

where $S = \{C, G\}$, represents BDS or GPS. The code hardware delay biases d_{rS} and d^S are assimilated into the clock offsets. The phase hardware delay biases b_{rS} and b^S are satellite-dependent and stable over time. They are absorbed by the corresponding ambiguity (Defraigne et al. 2007; Geng

et al. 2012; Jiang et al. 2015). In the formula (2), ISB is generally estimated over a period, such as a day or a period of data processed. It is found that ISB is extremely stable with time, and it is normally distributed approximately. The following parameters also need to be estimated in the equation.

$\widetilde{dt}_r$: the clock offset of station, one parameter to be estimated per epoch per station.

$\widetilde{N}_r^S$: the phase ambiguity, number of the parameters to be estimated depends on the number of satellites observed and the status of ambiguity. A network solution is applied where double-difference (DD) ambiguities are formed based on undifferenced (UD) ambiguity estimates and thus considerably improves the analysis efficiency (Ge et al. 2006; Geng et al. 2012).

ztd_r: ZTD, one parameter to be estimated for an hour of data processed.

The solution for combining multi-GNSS of BDS and GPS can be schematically illustrated with Fig. 3. The ZTD consists of the hydrostatic and wet components and both can be expressed by their individual zenith delay and mapping function. ZHD can be obtained more accurately (better than 1 mm) through the Saastamoinen model with the precise air pressure observation (Saastamoinen 1972), while the ZWD is the residual part to be estimated.

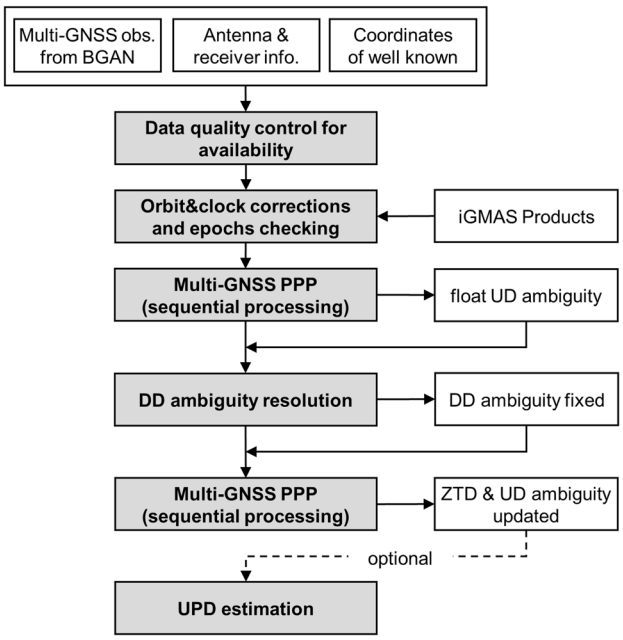

Fig. 3 The framework of the prototype multi-GNSS real-time PPP inversion system. As a national system, it can provide Uncalibrated Phase Delay (UPD) with an optional sequence

PWV inversion

There are three types of ZTD, which includes BDS-ZTD with BDS-only, GPS-ZTD with GPS-only, and Combined-ZTD with multi-GNSS of BDS and GPS. All these types of ZTD are retrieved through the PPP mode with the data from the BGAN, which can synchronously obtain data both of BDS and GPS. The PWV can be converted to when ZWD is accurately estimated.

$$\mathrm{PWV} = \prod \cdot \mathrm{ZWD} \tag{4}$$

$$\prod = 10^6 \times \left[\rho_{\mathrm{water}} R_{\mathrm{w}} \left(k_2' + \frac{k_3}{T_m}\right)\right]^{-1} \tag{5}$$

where $k_1 = 77.604\mathrm{K} \cdot \mathrm{hPa}^{-1}$, $k_2 = 64.79\mathrm{K} \cdot \mathrm{hPa}^{-1}$, and $k_3 = 377600\mathrm{K}^2 \cdot \mathrm{hPa}^{-1}$ are the physical constants, $\mathrm{k}_2' = \mathrm{k}_2 - \mathrm{k}_1(R_{\mathrm{d}}/R_{\mathrm{w}})$; $R_{\mathrm{d}} = 287.04\mathrm{J}/(\mathrm{kg} \cdot \mathrm{K})$, $R_{\mathrm{w}} = 461.5\mathrm{J} \cdot \mathrm{kg}^{-1}\mathrm{K}^{-1}$ and $\rho_{\mathrm{water}} = 1000\mathrm{kg} \cdot \mathrm{m}^{-3}$ are gas constant of dry air and water vapor, respectively; T_m can be estimated based on the ground temperature T_s, and usually $T_m = 70.2 + 0.72T_s$ (Davis et al.1985; Bevis et al. 1992). The ground temperature of each site come from the automatic meteorological instrument installed simultaneously with GNSS equipment when BGAN is built.

To ensure the integrity and continuity of PWV, a prior model of GPT (the Global Pressure and Temperature model) is used in ZTD estimation (Böhm et al. 2007; Lagler et al. 2013), and ZHD is calculated with air pressure from the prior models. The altitude difference between the meteorological equipment and the GNSS antenna is considered in the product inversion, which usually causes deviations in the meteorological parameters.

Water vapor products validation

The system can simultaneously obtain data both from BDS and GPS, and PWV products are retrieved every hour through the PPP mode, which includes three types, BDS-PWV with BDS-only, GPS-PWV with GPS-only, and Combined-PWV with multi-GNSS of BDS and GPS. The product validation is started with an introduction of data and data collocation principles. And GPS is a proven international application, and the comparison between PWV/BDS and PWV/GPS is significant for meteorological applications. Comparison with radiosonde is also presented in this section, and the characteristics of the results are also analyzed.

Basic principles of GNSS-PWV validation

This study estimates PWV products based on BGAN from 2018 to 2020 and the conventional radiosonde data during the same period. Radiosonde is the internationally standardized method for detecting high-altitude atmospheric elements, which can be used to verify the result of system inversion (Xia et al. 2021; Westwater 1997). The radiosonde data are obtained from the CMA, which could rapidly collect, exchange and distribute the regular radiosonde data internationally with the Global Telecommunication System (GTS) established by the World Meteorological Organization (WMO). The Manual on the Global Observing System (WMO 2015) prescribes that certain quality-control procedures must be applied to all meteorological data to be exchanged internationally. The CMA applies a series of checks to determine the quality of the radiosonde data under the recommendations of WMO (1950, 2017). The detailed procedures described in WMO (1993) are a guide to controlling the quality control of data for international exchange. The quality-control procedure is applied to check forcoding errors, internal consistency, time and space consistency, and physical and climatological limits (Marshal 2002; Lanzante 1996). The accuracy of radiosonde data is ± 0.5 K for temperature, ± 1 hPa for pressure, and ± 5% for humidity (WMO 1950, Durre et al. 2008).

The radiosonde directly measures meteorological elements such as temperature, humidity, and pressure along the ascent path of the sounding balloon carrying instruments, with daily observations made at 00:00 and 12:00 UTC. It is the internationally standardized method for detecting high-altitude atmospheric elements, which can be used to verify the result of system inversion (WMO 1950). The collocation principle is that the distance between the two stations of BGAN and radiosonde is less than 15 km, and there are 24 pairs as shown in bold red in Fig. 1. The radiosonde data include the temperature and dew point profiles of the atmosphere, and the water vapor pressure profile and PWV are calculated using (6) and (7), respectively.

$$e = 6.1078 \times 10^{\frac{7.69 t_d}{243.92 + t_d}} \tag{6}$$

$$\mathrm{PWV}_r = \frac{1}{\rho g} \int_0^{p_0} 0.622 \frac{e(k)}{p(k)} dp \tag{7}$$

where e is water vapor pressure, t_d is dew point (in degrees Celsius), PWV_r is the PWV calculated from radiosonde data, ρ is water density, g is gravitational acceleration, p is air pressure, and k is the number of atmosphere layer. The vertical height difference between the GNSS station and the radiosonde on the PWV is considered because PWV values are highly dependent on the elevation (Wang et al. 2017). The pressure, temperature and humidity of radiosonde data at the lower level are interpolated to the GNSS antenna height (Leckner 1978), and then the PWV is calculated from the antenna height with (7).

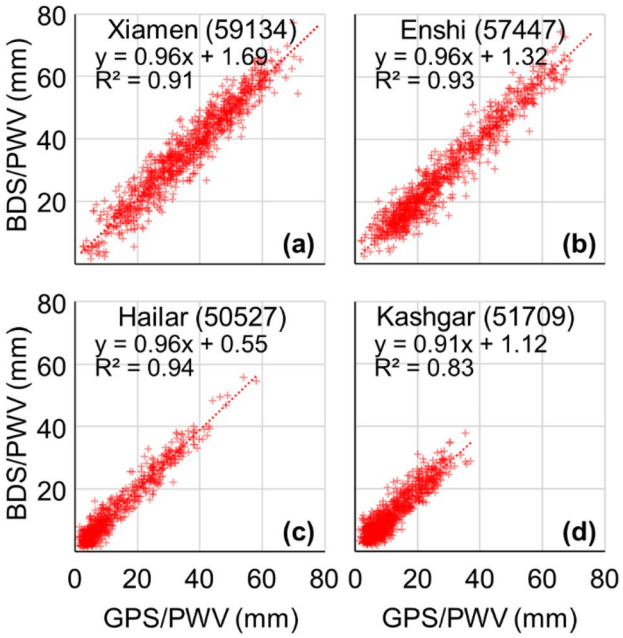

Fig. 4 Scatter plot of PWV between BDS and GPS at stations of Xiamen in Fujian **a**, Enshi in Hubei **b**, Hailar in Inner Mongolia **c**, Kashgar in Xinjiang **d**

PWV comparison between BDS and GPS solutions

As shown in Fig. 4, the scatter plot of BDS-PWV and GPS-PWV is shown from the Xiamen in Fujian province, Enshi in Hubei province, Hailar in Inner Mongolia autonomous region and Kashgar in Xinjiang Uygur autonomous region during the corresponding period of year 2018–2020, taking the more maturely used GPS as a reference. PWV results of BDS from the four stations are consistent with that of GPS, with the scatter points distributed along the $y=x$ line. The statistics for comparing BDS-PWV and GPS-PWV from the four stations are shown in Table 1. The bias between them is no more than 1 mm, with RMSE and Stdev ranging from 1.75 to 2.5 mm and RE ranging from 4.5 to 15%, all with correlation coefficients above 0.91. Depending on the location of the stations, it can be seen that the RE is smaller at stations with lower latitudes and lower altitudes due to climatic factors with larger PWV averages (Ave).

Three PWV products validation with radiosonde

A total of 24 stations collocated with the radiosonde are used for validation, as shown in bold red in Fig. 1. The biases,

Table 1 Comparison between BDS-PWV and GPS-PWV from four stations at Xiamen in Fujian, Enshi in Hubei, Hailar in Inner Mongolia and Kashgar in Xinjiang

Station	Altitude (m)	Bias (mm)	RMSE (mm)	Stdev (mm)	RE (%)	Corr	Ave (mm)
Xiamen	66.3	− 0.89	2.47	2.32	4.46	0.96	47.24
Enshi	473.6	− 0.13	1.97	1.97	6.27	0.97	37.23
Hailar	628.9	− 0.39	1.75	1.71	14.10	0.97	16.28
Kashgar	1241.4	0.82	2.50	2.38	14.93	0.91	17.03

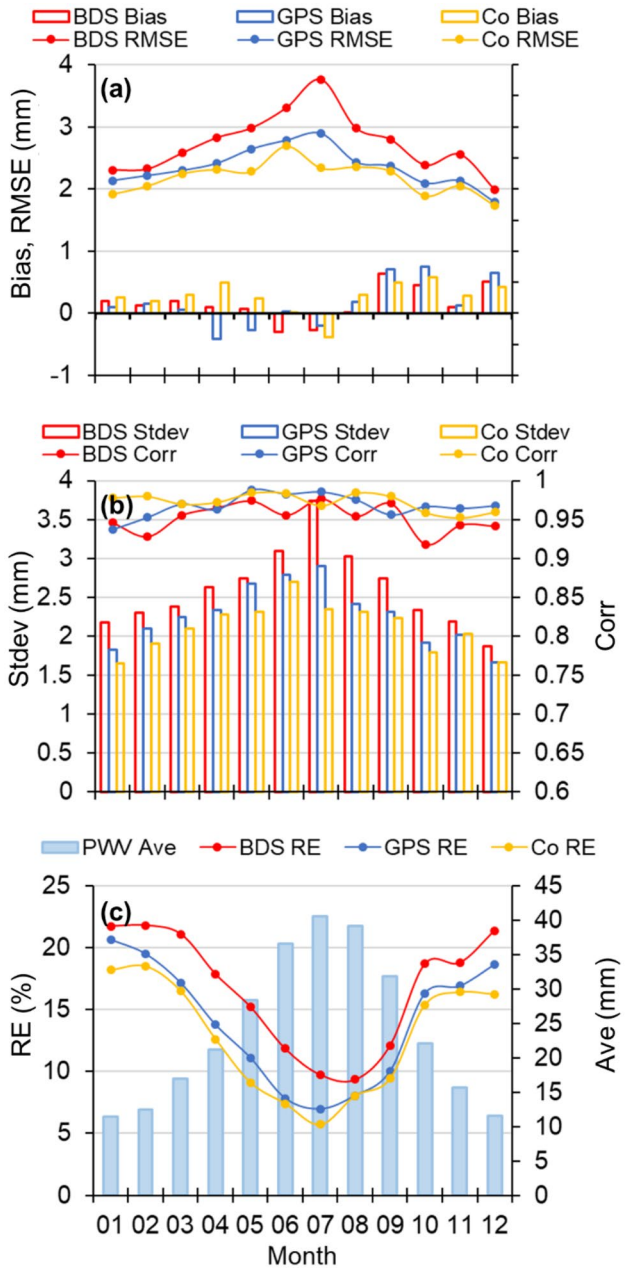

Fig. 5 Monthly statistics of three PWV products from BDS-only, GPS-only, and Combined BDS and GPS (Co). Bias and RMSE **a**; Stdev and Corr **b**; RE and PWV monthly average from radiosonde **c**

Table 2 Statistics of the three PWV products from BDS-only, GPS-only, and Combined BDS and GPS in 2018–2020

	Bias (mm)	RMSE (mm)	Stdev (mm)	RE (%)	Corr
BDS	0.15	2.73	2.60	16.64	0.95
GPS	0.16	2.35	2.27	13.91	0.97
Combined	0.27	2.18	2.11	12.80	0.97

RMSEs, REs, Stdevs, and Corrs (correlation coefficient) of the three products are calculated based on the radiosonde, as shown in Fig. 5. The biases and RMSEs of the three products usually follow the same trend with month (Fig. 5 top). Biases range from − 0.4 to 0.8 mm, with mostly positive biases, and the absolute biases are smaller in spring and summer and larger in autumn and winter. RMSEs range from 1.8 to 3.7 mm, with the largest in summer when there is more water vapor and the smallest in winter. BDS-PWV has the largest RMSE, followed by GPS-PWV, and Combined-PWV has the smallest RMSE. The Stdevs for the three products also have clear seasonal patterns similar to RMSEs, with the largest in summer and the smallest in winter. The three products all have high correlation coefficients, which are greater than 0.92 for all months, as shown in Fig. 5 (middle). RE varies from 5.7 to 21.7% (Fig. 5 bottom), with different characteristics from RMSE over the month, and it is minimal in summer. A possible explanation for this might be that PWV is much larger in summer than in other seasons. The largest average PWV is in summer months, with over 40 mm, approximately three times larger than in winter. BDS-PWV also has the largest RE of all three products, followed by GPS-PWV and the smallest of Combined-PWV.

Statistics of the three products from year 2018 to 2020 is shown in Table 2, compared to the radiosonde data. All the three products have positive mean biases but with small values. The overall BDS-PWV RMSE is 2.73 mm which is about 16% higher than that of GPS-PWV. But the Combined-PWV RMSE with multi-GNSS of BDS and GPS can be reduced by about 20%, which is better than both the results retrieved using BDS-only or GPS-only, and the same conclusion can be drawn from the statistical results of Stdev and RE. Their correlation coefficients with radiosonde are greater than or equal to 0.95, indicating a rather high correlation. The conclusion is consistent with the findings in Fig. 5.

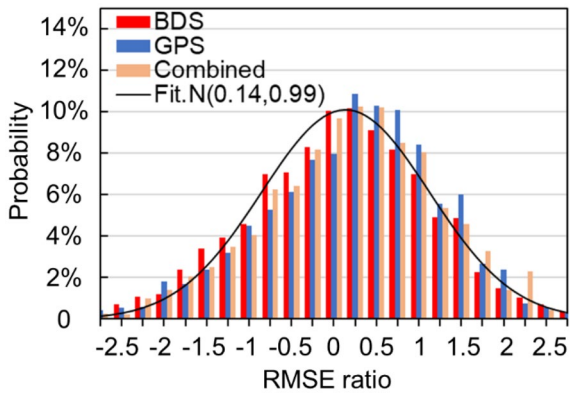

Fig. 6 Error probability densities of the three products (histogram shows the error probability densities of three products of PWV, and the black curve is of normally fitted, the abscissa represents the ratio of corresponding RMSE)

The error probability distribution for the three products according to corresponding RMSE ratios of each site (Fig. 6) tends to be normal, mostly concentrated between − 0.5 and 0.75 RMSE, accounting for about 60% of all samples. The mean bias and standard deviation of the three products are 0.14 and 0.99 RMSE, respectively, and the probability distribution with normally fitted is shown in the black curve in Fig. 6. The error probability distributions of the three products have positive biases compared to radiosonde data, with BDS-PWV having the smallest.

Figure 7 shows the statistics geographical distribution of three PWV products, which are retrieved with BDS-only, GPS-only, and Combined BDS and GPS. In terms of the distribution of bias, the regions of China with less water vapor in the west and north are mainly positive bias, while the regions with more water vapor in the south are mainly negative bias. The RMSE is mostly around 2 mm, with higher RMSE values exceeding 3 mm in areas with higher water vapor content in southeast China. The BDS-PWV RMSE of most stations are the highest of the three types of products, while Combined-PWV has the lowest RMSE. The correlation coefficients between the three products and radiosonde are relatively high, and most stations of the three products are basically higher than 0.9. The correlation coefficient is the lowest for BDS-PWV at most stations, and the largest for Combined-PWV with BDS and GPS. This is consistent with the conclusion in Fig. 5.

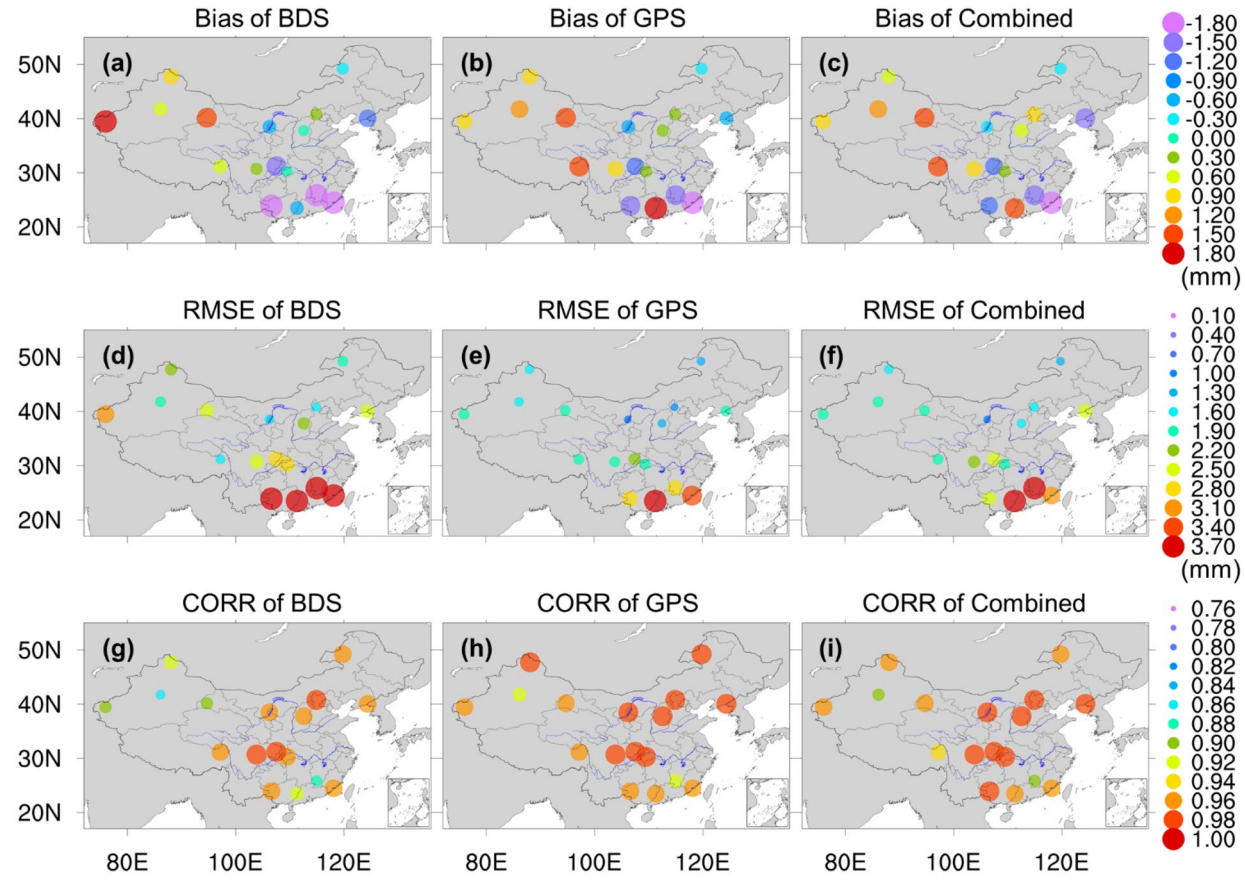

Fig. 7 Statistics geographical distribution of three PWV products from BDS-only, GPS-only, and Combined BDS and GPS

Conclusions and discussions

The meteorological application system based on BGAN, adopting a systematic construction approach, is carried out to effectively coordinate GNSS and ground resources and promote the high-quality development of BDS meteorological industry service. The synchronization of BDS and GPS and real-time observation of the atmosphere are carried out nationwide in China, retrieving atmospheric water vapor with multi-GNSS application. Through the multi-GNSS data combination and its water vapor products validation, PWV estimated with BDS-only is equivalent to that with GPS, which is more mature in international applications. The RMSE is about 2 mm, and the correlation coefficient is higher than 0.95. Based on radiosonde data, validation is conducted on the three products of BDS-PWV, GPS-PWV, and Combined-PWV. It is found that the error characteristics of the three products showed a consistent trend over the months. The PWV bias of the three products was relatively small, with RMSE of 2.18–2.73 mm. Among them, BDS-PWV has the largest RMSE, followed by GPS-PWV, and Combined-PWV has the smallest RMSE. However, the Combined-PWV with multi-GNSS of BDS and GPS can be improved by about 20%, which is better than both the results retrieved using BDS-only or GPS-only.

As the latest development in the GNSS infrastructure of China, BGAN contributes to atmospheric water vapor observation and multi-GNSS applications. In future, the development of the BGAN will promote the construction of high-density station networks and the improvement of high-precision positioning technology. The construction of the integrated system based on BGAN is continuing to promote, with the application of technologies such as multi-GNSS combination, low earth orbit satellite occultation, and GNSS reflection in the meteorological service.

Acknowledgements We are grateful to the Wuhan University and iGMAS for providing open GNSS data. Finally, we would like to thank Dr. George Zhizhao Liu from Hong Kong Polytechnic University, Dr. Weixing Zhang from Wuhan University and Dr. Min Liu from Shanghai Meteorological Service for their valuable comments and suggestions.

Authors contributions DU: Conceptualization, Methodology, Formal analysis, Writing and Funding acquisition. CAO: Project administration, Data collection. L: Supervision, Data collection, Funding acquisition, Writing—review & editing. HWS and JIAO: Resources, Writing—review & editing.

Funding Supported by the Natural Science Foundation of Shanghai Science Technology Commission (23ZR1447300), the National Natural Science Foundation of China (42174027), the Guangxi Key research and development program (GUIKEAB21075005), the Innovation and Development Foundation of China Meteorological Administration (CXFZ2024J061).

Data availability The GNSS observational data can be made available upon request by applying to the Meteorological Observation Center of China Meteorological Administration or contacting the authors.

Declarations

Competing interests The authors declare no competing interests.

Consent for publication All authors approved the final manuscript and the submission to this journal.

References

Bevis M, Businger S, Herring TA, Rocken C, Anthes RA, Ware RH (1992) GPS meteorology: remote sensing of atmospheric water vapor using the global positioning system. J Geophys Res Atmos 97(D14):15787–15801. https://doi.org/10.1029/92jd01517

Böhm J, Niell A, Tregoning P, Schuh H (2006) Global mapping function (GMF): a new empirical mapping function based on numerical weather model data. Geophys Res Lett 33(7):1–4. https://doi.org/10.1029/2005GL025546

Böhm J, Heinkelmann R, Schuh H (2007) Short note: a global model of pressure and temperature for geodetic applications. J Geod 81(10):679–683. https://doi.org/10.1007/s00190-007-0135-3

Bu JW, Yu KG, Qian NJ, Zuo XQ, Chang J (2021) Performance assessment of positioning based on multi-frequency multi-GNSS observations: signal quality, PPP and baseline solution. IEEE Access 9:5845–5861. https://doi.org/10.1109/access.2020.3048352

Cai HL, Chen G, Jiao WH, Chen KK, Xu TH, Wang HC (2016) An initial analysis and assessment on final products of iGMAS. In: Sun J D, Liu J N, Fan S W, Wang F X (eds) China satellite navigation conference (CSNC) 2016 proceedings: volume III. Lecture notes in electrical engineering, vol 390. Springer, Singapore. https://doi.org/10.1007/978-981-10-0940-2_45

Chen QM, Song SL, Zhou WL (2021) Accuracy analysis of GNSS hourly ultra-rapid orbit and clock products from SHAO AC of iGMAS. Remote Sens 13(5):1022. https://doi.org/10.3390/rs13051022

Davis JL, Herring TA, Shapiro II, Rogers AE, Elgered G (1985) Geodesy by radio interferometry: effects of atmospheric modeling errors on estimates of baseline length. Radio Sci 20(6):1593–1607

Defraigne P, Baire Q, Guyennon N (2007) GLONASS and GPS PPP for time and frequency transfer. In: IEEE International frequency control symposium joint with the 21st European frequency and time forum, Geneva, Switz. https://doi.org/10.1109/FREQ.2007.4319211

Durre I, Menne MJ, Vose RS (2008) Strategies for evaluating quality assurance procedures. J Appl Meteor Climatol 47(6):1785–1791. https://doi.org/10.1175/2007JAMC1706.1

El-Mowafy A, Deo M, Rizos C (2016) On biases in precise point positioning with multi-constellation and multi-frequency GNSS data.

Meas Sci and Technol 27(3):035102. https://doi.org/10.1088/0957-0233/27/3/035102
Federal Aeronautics Administration (FAA) (2017) Satellite navigation—GBAS—how it works. https://www.faa.gov/about/office_org/headquarters_offices/ato/service_units/techops/navservices/gnss/laas/howitworks
Ge M, Gendt G, Dick G, Zhang FP, Rothacher M (2006) A new data processing strategy for huge GNSS global networks. J Geod 80:199–203. https://doi.org/10.1007/s00190-006-0044-x
Geng JH, Shi C, Ge MR, Dodson AH, Lou YD, Zhao QL, Liu JN (2012) Improving the estimation of fractional-cycle biases for ambiguity resolution in precise point positioning. J Geod 86(8):579–589. https://doi.org/10.1007/s00190-011-0537-0
Geng JH, Zeng R, Guo J (2024) Assessing all-frequency GPS/Galileo/BDS PPP-RTK in GNSS challenging environments. GPS Solut 28:5. https://doi.org/10.1007/s10291-023-01543-0
Guo QY, Hou JH, Chen SH, Sun YJ (2020) Near real-time detecting of atmospheric water vapor content based on BeiDou Navigation Satellite System. J Phys Conf Ser 1654:012125. https://doi.org/10.1088/1742-6596/1654/1/012125
Jiang P, Ye SR, Liu YY, Zhang JJ, Xia PF (2014) Near real-time water vapor tomography using ground-based GPS and meteorological data: Long-term experiment in Hong Kong. Ann Geophys 32(8):911–923. https://doi.org/10.5194/angeo-32-911-2014
Jiang N, Xu Y, Xu TH, Xu GC, Sun ZZ, Schuh H (2015) GPS/BDS short-term ISB modelling and prediction. GPS Solut 21(1):1–13. https://doi.org/10.1007/s10291-015-0513-x
Jones J, Guerova G, Dousa J, Dick G, Haan S, Pottiaux E, Bock O, Pacione R, Malderen R (2020) COST action ES1206: advanced GNSS tropospheric products for monitoring severe weather events and climate. Springer Nat Switz AG. https://doi.org/10.1007/978-3-030-13901-8
Kazmierski K, Zajdel R, Sośnica K (2020) Evolution of orbit and clock quality for real-time multi-GNSS solutions. GPS Solut 24(4):111. https://doi.org/10.1007/s10291-020-01026-6
Kee C, Park S, Yun Y (2004) Comparative study between GBAS and conventional aircraft precision approach guidance system. Trans Jpn Soc Aeronaut Space Sci 46(154):224–229. https://doi.org/10.2322/tjsass.46.224
Kouba J (2009) A guide to using international GNSS service (IGS) products. http://igscb.jpl.nasa.gov/igscb/resource/pubs/UsingIGSProductsVer21.pdf
Lagler K, Schindelegger M, Böhm J, Krásná H, Nilsson T (2013) GPT2: empirical slant delay model for radio space geodetic techniques. Geophys Res Lett 40(6):1069–1073. https://doi.org/10.1002/grl.50288
Lanzante JR (1996) Resist ant, robust and non-parametric techniques for the analysis of climate data: theory and examples, including applications to historical radiosonde station data. Int J Climatol 16(11):1197–1226. https://doi.org/10.1002/(SICI)1097-0088(199611)16:11%3C1197::AID-JOC89%3E3.0.CO;2-L
Leckner B (1978) The spectral distribution of solar radiation at the earth's surface—elements of a model. Sol Energy 20(2):143–150. https://doi.org/10.1016/0038-092X(78)90187-1
Li M, Li WW, Shi C, Zhao QL, Su X, Qu LZ, Liu ZZ (2015a) Assessment of precipitable water vapor derived from ground-based BeiDou observations with precise point positioning approach. Adv Space Res 55(1):150–162. https://doi.org/10.1016/j.asr.2014.10.010
Li XX, Ge MR, Dai XL, Ren XD, Fritsche M, Wickert J, Schuh H (2015b) Accuracy and reliability of multi-GNSS real-time precise positioning: GPS, GLONASS. Beidou Galileo J Geod 89(6):607–635. https://doi.org/10.1007/s00190-015-0802-8
Li XX, Zus F, Lu CX, Dick G, Ning T, Ge MR, Wickert J, Schuh H (2015c) Retrieving of atmospheric parameters from multi-GNSS in real time: validation with water vapor radiometer and numerical weather mode. J Geophys Res Atmos 120(14):7189–7204. https://doi.org/10.1002/2015JD023454
Li XX, Tan H, Li X, Dick G, Wickert J, Schuh H (2018) Real-time sensing of precipitable water vapor from BeiDou observations: Hongkong and CMONOC networks. J Geophys Res Atmos 123(15):7897–7909. https://doi.org/10.1029/2018JD028320
Liang H, Cao YC, Wan XM, Xu ZF, Wang HS, Hu H (2015) Meteorological applications of precipitable water vapor measurements retrieved by the national GNSS network of China. Geod Geodyn 6(2):135–142. https://doi.org/10.1016/j.geog.2015.03.001
Lou YD, Zheng F, Gu SF, Wang C, Guo HL, Feng YM (2016) Multi-GNSS precise point positioning with raw single-frequency and dual-frequency measurement models. GPS Solut 20(4):849–862. https://doi.org/10.1007/s10291-015-0495-8
Lu CX, Li XX, Nilsson T, Ning T, Heinkelmann R, Ge MR, Glaser S, Schuh H (2015) Real-time retrieval of precipitable water vapor from GPS and BeiDou observations. J Geod 89(9):843–856. https://doi.org/10.1007/s00190-015-0818-0
Marshall GJ (2002) Trends in Antarctic geopotential height and temperature: a comparison between radiosonde and NCEP–NCAR reanalysis data. J Clim 15(6):659–674. https://doi.org/10.1175/1520-0442(2002)015%3C0659:TIAGHA%3E2.0.CO;2
Montenbruck O, Steigenberger P, Prange L, Deng ZG, Zhao QL, Perosanz F et al (2017) The multi-GNSS experiment (MGEX) of the International GNSS service (IGS)—achievements, prospects and challenges. Adv in Space Res 59(7):1671–1697. https://doi.org/10.1016/j.asr.2017.01.011
Mota GV, Song SL, Stpniak K (2019) Assessment of integrated water vapor estimates from the iGMAS and the Brazilian network GNSS ground-based receivers in Rio de Janeiro. Remote Sens 11(22):2652. https://doi.org/10.3390/rs11222652
Pinker A, Smith C, Day J (2000) Wide-area augmentation system (WAAS)—the metamorphosis of a major FAA program. GPS Solut 3(3):48–57. https://doi.org/10.1007/PL00012815
Prange L, Orliac E, Dach R, Arnold D, Beutler G, Schaer S, Jäggi A (2017) CODE's five-system orbit and clock solution—the challenges of multi-GNSS data analysis. J Geod 91(4):345–360. https://doi.org/10.1007/s00190-016-0968-8
Saastamoinen J (1972) Contributions to the theory of atmospheric refraction. Bull Géod 105(1):279–298. https://doi.org/10.1007/bf02521844
Wang Y, Yang K, Pan ZY, Qin J, Chen DL, Lin CG et al (2017) Evaluation of precipitable water vapor from four satellite products and four reanalysis datasets against gps measurements on the southern tibetan plateau. J Clim 30(15):5699–5713. https://doi.org/10.1175/JCLI-D-16-0630.1
Westwater E (1997) Remote sensing of tropospheric temperature and water vapor by integrated observing systems. Bull Am Meteorol Soc 78(9):1991–2006. https://doi.org/10.1175/1520-0477-78.9.1991
WMO (1950) Guide to instruments and methods of observation (WMO-No.8), Volume I and V, Geneva, Switz. https://library.wmo.int/idurl/4/41650
WMO (1993) Guide on the global data-processing system (WMO-No.305), Geneva, Switz. https://library.wmo.int/idurl/4/28978
WMO (2015) Manual on the global observing system (WMO-No.544), Volume I, Geneva, Switz. https://library.wmo.int/idurl/4/58672
WMO (2017) Guide to the implementation of quality management systems for national meteorological and hydrological services and other relevant service providers (WMO-No.1100), Geneva, Switz. https://library.wmo.int/idurl/4/50552
Xia PF, Ye SR, Xu CJ, Jiang WP (2021) Establishing a high-precision ZHD model of China using 8 years of radiosonde data. J Atmos Ocean Technol 38(6):1173–1186. https://doi.org/10.1175/JTECH-D-20-0173.1

Xu AG, Xu ZQ, Ge MR, Xu XC, Zhu HZ, Sui X (2013) Estimating zenith tropospheric delays from BeiDou navigation satellite system observations. Sens 13(4):4514–4526. https://doi.org/10.3390/s130404514

Zhang WX, Lou YD, Gu SF, Shi C, Haase JS, Liu JN (2016) Joint estimation of GPS/BDS real-time clocks and initial results. GPS Solut 20(4):665–676. https://doi.org/10.1007/s10291-015-0476-y

Zhang WX, Lou YD, Cao YC, Liang H, Shi C, Huang JF, Liu WX, Zhang Y, Fan BB (2019) Corrections of radiosonde-based Precipitable water using ground-based GPS and applications on historical radiosonde data over china. J Geophys Res: Atmos 124(6):3208–3222. https://doi.org/10.1029/2018JD029662

Mingbin Du is responsible for the construction of GNSS/MET network in Shanghai, China. He has been engaged in research and operation on GNSS/MET and promoting the integration and application of the network. Over 200 stations in East China were integrated to form the largest regional real-time GNSS network in China. His research interests include GNSS/MET and satellite remote sensing.

Yunchang Cao is responsible for the GNSS/MET innovation team of CMA, designing and operating the China GNSS/MET network. His team is in charge of the GNSS meteorological demonstration project–the BeiDou meteorological application in the atmospheric, marine and space weather. Currently, they are working on the operation and the study of the BeiDou-based GNSS/MET application in CMA.

Hong Liang earned a PhD degree in meteorology from the University of Chinese Academy of Sciences in 2012. He was a visiting scholar at the Scripps Institution of Oceanography, University of California San Diego, USA, from 2017–2018. He is currently a researcher with the Meteorological Observation Center of CMA. His main research interests are GNSS-refractometry and GNSS-reflectometry.

Heng Hu is a senior scientist at the China Meteorological Administration. Her main research areas are weather radar data quality control and GNSS/MET observation techniques. She has published 9 papers in core journals in the past five years. Her research interests include GNSS application and meteorological observation.

Haishen Wang has been engaged in research and operation work on GNSS/MET applications for a long time. He designed and established GNSS/MET business network of the China Meteorological Administration, evaluated the performance of PWV measured by ground-based GNSS and radiosonde, and made a detailed comparative analysis among Beidou, GPS and radiosonde. His research interests include GNSS application and data assimilation.

Shuli Song is currently a professor at the Shanghai Astronomical Observatory, Chinese Academy of Sciences, Shanghai, China. Her main research interests are GNSS data processing and application.

Guoqiang Jiao received a Ph.D. degree at University of Chinese Academy of Sciences, China. His main research interests are satellite clock estimation and its applications.